International Journal of Geotechnical Earthquake Engineering
Volume 11 • Issue 2 • July-December 2020

Liquefaction Susceptibility Assessment Using Geotechnical and Geological Manners of Northern Thailand

Yayat Kusumahadi, Kasetsart University, Thailand
Suttisak Soralump, Kasetsart University, Thailand
Montri Jinagoolwipat, Electricity Generating Authority of Thailand, Thailand

ABSTRACT

Soil site investigations such as boring logs, basic soil properties, spectral analysis of surface wave, and the examinations of geologic and geomorphologic were performed in Mae Lao area to investigate the susceptibility of liquefaction after the 6.2 Mw Chiang Rai Earthquake 2014. The study area was found to lay on a complex geological formation and geotechnical behavior with a condition of the high groundwater table. Being located on a high seismicity area (intensity V-VII Mercalli) governs the study area as a concern for high liquefaction hazards. Liquefaction susceptibility-based compositional criteria, soil resistance, and geologic criteria have been established, and consequently, the character of liquefaction potential is defined.

KEYWORDS

Earthquake, Geological Liquefaction, Liquefaction Potential, Liquefaction Susceptibility, Seismic Hazard

1. INTRODUCTION

Liquefaction is the phenomena related to the earthquake shaking, as causes of increasing of pore water pressure and induced loss of shear resistance in granular soils. The susceptibility of liquefaction is controlled several of factors including grain size distribution (texture), soil density, depth to groundwater and the liquefaction triggering threshold with concerning the level of ground shaking that might be anticipated for the study area (Pyke, 2003). The texture and soil density are strongly influenced by the depositional system and deposit age, which allow the correlation between the characteristic of a Quaternary deposit with soil gradation, soil properties, and the level of ground shaking. The Northern part of Thailand was hit by an earthquake of magnitude 6.2 M_w Chiang Rai earthquake on May 5, 2014. This event has one of the most significant effects on the social community and human lives in the hazard area causing several damages such as liquefaction, landslides, and other associated ground failures. The epicenter was located in the Phayao fault zone ranging from northeast to southeast of Mae Lao District, Chiang Rai Province, at Latitude 19.750ºN and Longitude 99.690ºE with the focal depth of epicenter is approximately 10 km (TMD, 2014). Some zones were affected by liquefaction within a radius of 20 km from the epicenter shown in Figure 1. From the

DOI: 10.4018/IJGEE.2020070103

Figure 1. (a) Liquefaction at the edge of the road, (b) liquefaction-induced soil boiling (c) liquefaction on the paddy field

soil investigation, it was determined that the soil layers of some boreholes consist of a poorly graded loose saturated sand layer in the shallow depth from the ground surface. Hence, some settlements of shallow foundation and structural damage were observed induced by the liquefaction although it is not serious damage. Moreover, the geological and geotechnical considerations of the study area which were investigated previously indicated the evidence of the liquefiable material are susceptible to liquefaction.

The depositional mechanism controls the texture, sorting, and packing of sediments (Youd & Perkins, 1978). Investigation of the study area including borehole log measurement, spectral analysis of surface wave, observation well, and examination of the geological surface have been established to assess the liquefaction susceptibility of the study area. The investigation focuses on the Mae Lao area where the high seismic and ground failure hazards occurred after the 2014 earthquake. All those measurements were conducted in both locations where the liquefaction was experienced (eyewitness evidence) and the area without evidence of liquefaction. Furthermore, the site class of particular locations has been defined in this study. In general, the results brought an understanding of the effect of geotechnical and geological conditions on the liquefaction susceptibility and the soil behavior under the event of 6.2 M_w Chiang Rai Earthquake 2014.

2. STUDY AREA

Figure 2 shows the exact location of the study area which is located in Mae Lao district, Chiang Rai Province, Northern part of Thailand close to the Myanmar and Laos borders. The area was found to lay

Figure 2. Location of the study area (Source: GERD, 2020)

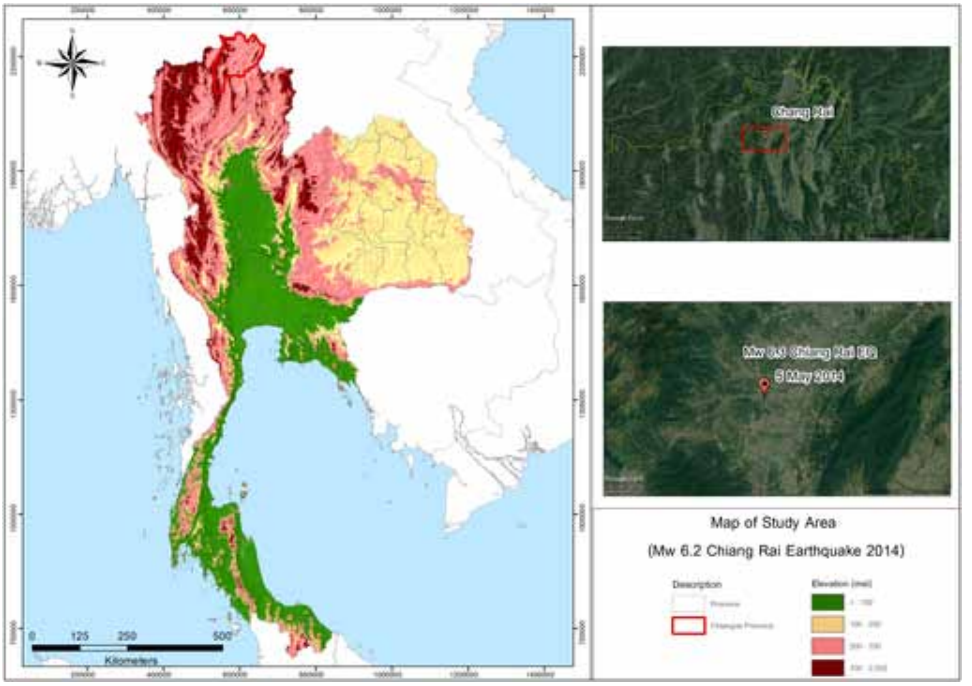

on a complex geological formation, the middle part is composed of deposited sediment of Quaternary deposit alluvium (Q_a), Terrace (Q_t), Floodplain (Q_{ff}) which is known to have a medium-to-high potential of liquefaction. Additionally, some of the mountainous areas were dominated by Sandstone (CP) at stations BH8 and BH13, and volcanic basic rocks (SD) at station 9 along the northern-western part (Figure 3). These types of sediment deposition affect varying liquefaction behavior. Therefore, to describe the character of each type, further investigations were carried out by performing such as Standard Penetration Test (SPT) to define the liquefaction behavior due to the compositional criteria and solve the liquefaction potential prediction. Moreover, observation well was performed to monitor the influence of groundwater level and overburden pressure.

2.1 Deposit Soil Layer

As shown in Figure 3, Mae Lao district has several types of geological profiles. Fifteen points were selected according to the deposit characteristics and liquefied or non-liquefied soils in the study area, as well as the spectral analyses of surface wave (SASW) tests. They were performed to represent the geotechnical characteristic of the deposit soil layer, which further to be associated with the geological aspects in terms of assessment of liquefaction susceptibility. Based on the observation, it was found that BH1 to BH11 (except BH8 and BH9) consist of saturated loose sand layer, and borehole 12 to 15 consist of medium dense to dense deposit material.

Thai Department of Mineral Resource (TDMR) reported that there was liquefaction evidence in Mae Suai, Phan, and Mae Lao Districts (Figure 1). Moreover, the locations of liquefaction evidence located on Quaternary sediment area including late Holocene alluvial (Q_a), Late Pleistocene-Holocene Terrace (Q_t), and Alluvial fan deposits (Q_{ff}). The location where the liquefaction evidence was found, typically located in the area of Quaternary sediment which is susceptible to liquefaction. Therefore, the location of the borehole in this study is scattered. The locations of boreholes and characteristics of soil layers are shown in Figure 7 and Table 1.

Figure 3. Geological map and geotechnical exploration points of Mae Lao District, Chiang Rai, Thailand (Scale 1:100,000) (Source: adapted from Geological Map of presented by TDMR, 1990)

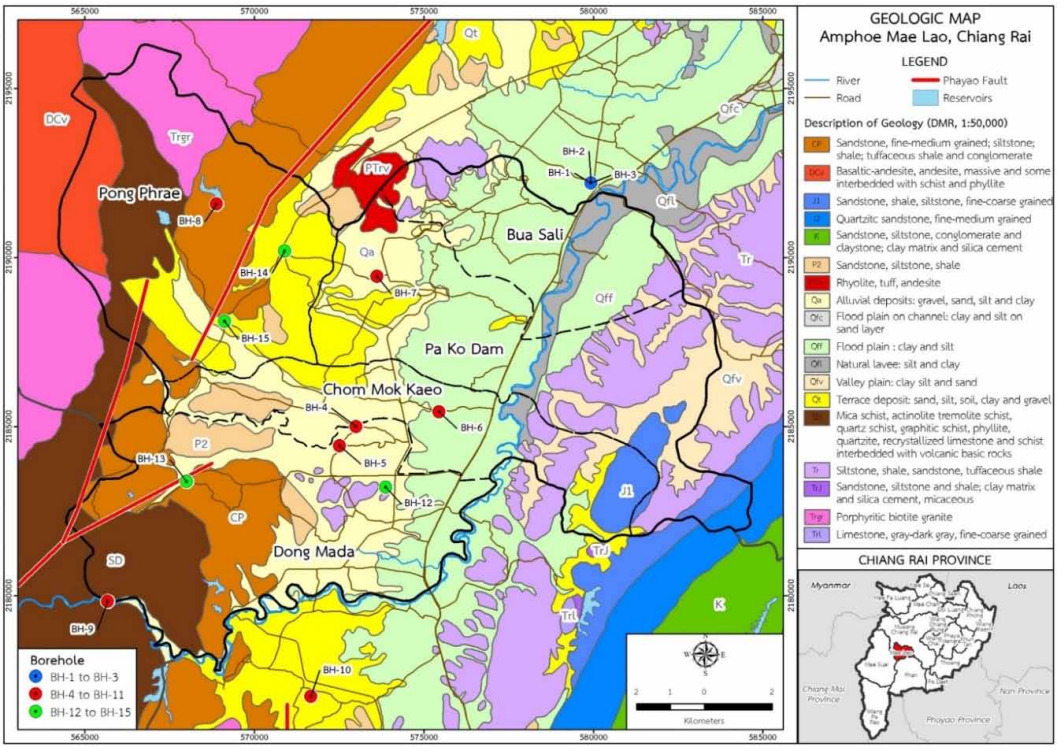

2.2 Shear Wave Velocity Profile

One of the key parameters that must be defined is the shear wave velocity (V_S). This parameter is a valuable indicator of the dynamic properties of soil in its relationship with the maximum shear modulus (G_{max}). Tangjittham (2017) performed the spectral analysis of surface wave (SASW) in 14 locations (same with borehole location as shown in Figure 3) from station V_{S1} to V_{S15} (except V_{S2} which is approximately only 10 m away from V_{S1} and assumed similar behavior). From the observation, it was found that the value of averaged shear wave velocity on top of 30 m (V_{S30}) is approximately ranging between 250 to 500 m/s and has been classified as site class C and D according to the NEHRP classification system (Table 2).

Since SASW could not reach the maximum depth of 30 km, the proposed method from Boore (2004) was adapted for extrapolation that extended to a depth of at least 30 m based on a regression analysis of 135 boreholes in California. This model involves a statistical relation between V_{S30} and the time-averaged to the terminal depth of measurement (V_{Sd}). Regression coefficients are ranging for the depth of 10 to 29 m. For some stations that did not reach 10 m such as V_{S1}, V_{S8}, and V_{S14}, they were assumed to be close to 10 m, having the same regression coefficient:

$$\log V_{S30} = a + b \times \log V_{sd} \tag{1}$$

where a and b are regression coefficients. Correlation coefficient (r) between V_{Sd} and V_{S30} for the dataset are presented in Boore (2011) for the depths of 5 m (r = 0.75), 10 m (r = 0.92), 15m (r =

Table 1. Characteristic of the soil layer in the study area

Station	Coordinates		Quaternary Type	Geotechnical Characteristic (USCS)
	Lat. (N)	Long. (E)		
BH 1	19.82421	99.76320	Q_{ff}	2 m of Silty Sand (SM), 4 m of Silty Clay (CH), 1 m of Silty Clay (CH), and 7 m of Dense Silty Sand some Gravel (SM). Boring ended at 14.45 m
BH 2	19.82421	99.76289	Q_{ff}	8 m of Sandy and Silty Clay (CL), 2 m of Loose Silty Sand (SM), and 9 m of Dense Silty Sand some Gravel (SM). Boring ended at 17.45 m.
BH 3	19.82451	99.76310	Q_{ff}	3 m of Silty Clay (CL), 2 m Silty Clay (CH), 1 m Very Loose Silty Sand (SM), and 7 m of Dense Silty Sand. Boring ended at 13.45m.
BH 4	19.75961	99.69688	Q_a	2 m of Loose Silty Sand (SM), 5 m of Sandy and Clayey Silt (ML), 2 m of Silty Gravel (GM), Dense silty Sand (SM) and Silty Gravel (GM). Boring ended at 11.15 m.
BH 5	19.75439	99.69211	Q_a	2 m of Silty Clay (SM), 2 m of Clayey Sand, 1 m of loose silty Sand, 2 Dense silty Sand (SM), 2 m of Silty Gravel (GW_GM), and 4 m of Silty Sand (SM). Boring ended at 14.10 m.
BH 6	19.76337	99.72059	Q_{ff}/Q_a	4 m of Sandy Silt (ML), 2 m of Silty Sand (SW-SM), 1 m of Loose Sand (SP-SM), 2 m of Sandy Clay (CL), 1 m Clayey Sand, 4 m of Clayey Silt (ML), and 3 m of Silty Sand (SM). Boring ended at 17.45
BH 7	19.79962	99.70361	Q_a	3 m of Sandy Clay (CL), 2 m of Loose to very Loose Clayey Sand (SC), 3 m of Sandy Clay (CH), 2 m of Silty Sand (SM), 2 m of Sandy Silt (ML), 2 m of Very Dense Silty Sand (SM). Boring ended at 16.45
BH 8	19.81991	99.65781	CP	4 m of Sandy Silt (ML), 2 m of Sandy Clay (CL), 2 m of Silty Gravel (GM), Boring log ended at depth of 8 m.
BH 9	19.71367	99.62831	SD	8 m thick of Silty Clay (CL), 2 m of silty Sand, boring log Bedrock found at 11 m.
BH 10	19.68779	99.68379	Q_t	2 m of Silty Clay (CL), 4 m of Silty Sand (1 loose SM, 1 Dense SP-SM, and 2 Dense SW-SM), 2 m of Poorly Graded sand, 6 m of Silty Sand, Boring ended at 13.30 m.
BH 11	19.64923	99.50963	Q_a	2 m of Silty Sand (SM), 1 m of Silty Clay (CL), 2 m of Loose Clayey Sand (SC), 1 m of Very Loose Silty Sand (SM), 3 m of Sandy Clay (CL), 1 m of Poorly Graded Sand (SP), very Dense Silty Sand (SM), Boring ended at 12.45 m
BH 12	19.74342	99.70494	T_r	5 m of Sandy Clay (CL), 2 m of Clayey Silt (MH), 3 m of Sandy Clay (CL), 2 m of Clayey Silt (MH), 2 m of Sandy Silt (ML), 2 m of Silty Sand (SM), Boring ended at 14.15 m.
BH 13	19.74404	99.66323	CP	3 m of Sandy Clay (CL), 1 m of Silty Clay (CL), 1 m of Clayey Gravel (GC), 2 m of Dense Clayey Sand (SC), Bedrock found at 7 m
BH 14	19.80651	99.67614	Q_t	2 m of Sandy Silt (ML), 3 m of Silty Sand (SM), 1 m of Sandy Silt (ML), 1 m of Very dense Silty Gravel (GM).
BH 15	19.78741	99.65978	CP/Q_t	3 m of Clayey Silt (ML), 1 m of Silty Sand (SM), 3 m of Sandy Silt (MH), 3 m of Silty Clay (CL), and 2 m of Clayey Silt (ML). Boring ended at 12.28 m.

Figure 4. Soil strata of BH10 station

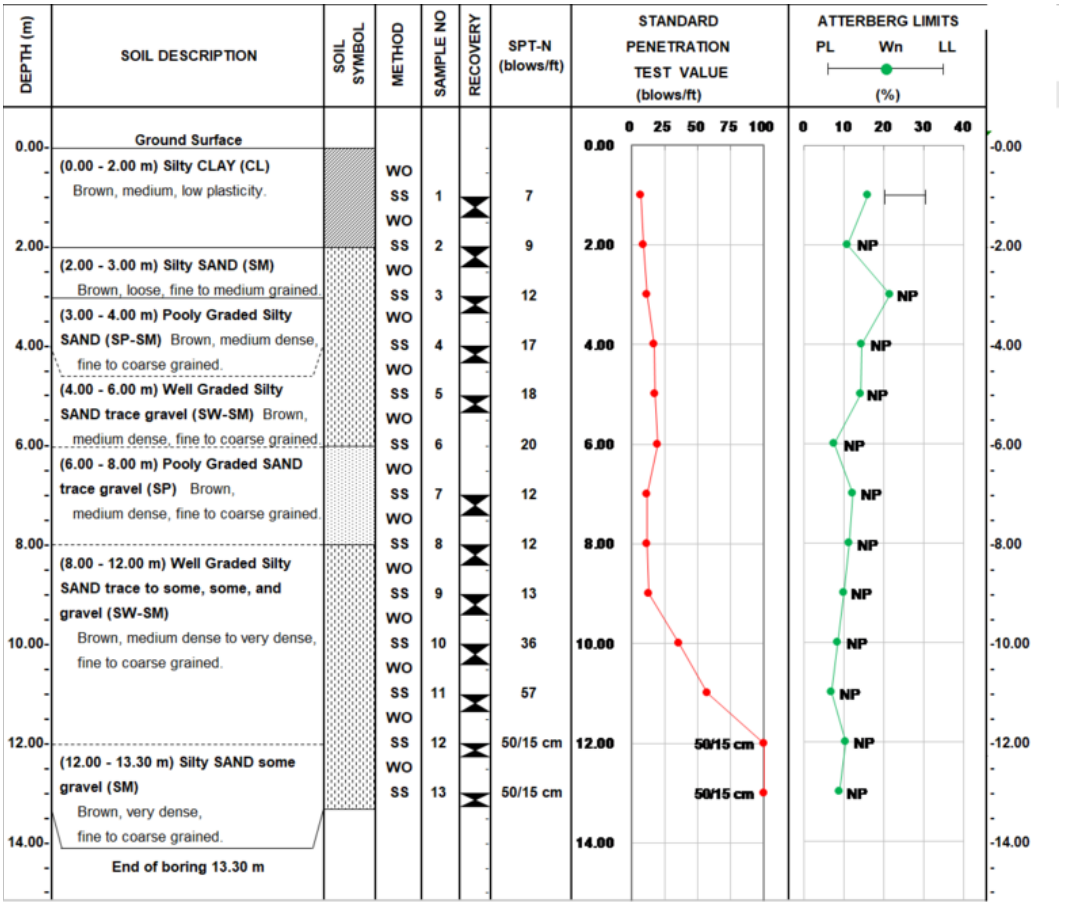

0.92), and 20 m (r = 0.99). As expected, correlation becomes stronger as the depth of measurement approaches 30 m.

3. SEISMOLOGICAL CHARACTERISTIC

Department of Mineral Resource associated with the Thai Meteorological Department and National Earthquake Information Center has created a seismic hazard zoning map of Thailand to present the earthquake intensity in every zone as a reference for the design code. The study area is located in zone 2B with the earthquake intensity V-VII Mercalli scale and the severity is slight to moderate damage for well-built ordinary structure.

The study area is located in the South-East Asia (SEA) region, on the boundary of the Indo-Australian and Eurasian plates. The Indo-Australian and Eurasian boundary zone comprise of the convergent margins, including Burma oblique subduction zone, Andaman thrust, and Sunda arc, to the northwest, west, and south, respectively (Ornthammarath & Warnitchai, 2016). As reported by McCaffrey (1996), the convergence rate of Australia moving toward SEA is about 65-70 mm/year. One of the past 2004 earthquakes in South-East Asia was caused by the subduction activity of both plates of the Sumatra Megathrust earthquake (Ammon et al., 2005). A consequence of India drove into the southern margin of Eurasia, Indochina was rotated clockwise about 25° and extruded to the

Figure 5. Equipment used for SASW measurement (a) Sledgehammer (b) drop weight (c) two geophone receivers (d) spectrum analyzer

Table 2. V_{S30} prediction of study area

Station	End Depth of Reading (h_d)	Regression Coefficient		V_{sd}	V_{S30}	Site Class (NEHRP)
		a	b	(m/s)	(m/s)	
Vs1	8	0.042062	1.0292	255.748	331.27	D
Vs2	-	-	-	-	-	-
Vs3	20	0.025439	1.0095	306.805	343.50	D
Vs4	18	0.024879	1.0144	307.087	353.15	D
Vs5	26	0.006565	1.0045	316.516	329.77	D
Vs6	18	0.024879	1.0144	260.587	298.97	D
Vs7	27	0.002519	1.0043	262.465	270.39	D
Vs8	8	0.042062	1.0292	253.053	327.68	D
Vs9	20	0.025439	1.0095	279.408	312.545	D
Vs10	26	0.006565	1.0045	256.969	276.83	D
Vs11	27	0.002519	1.0043	304.338	313.73	D
Vs12	26	0.006565	1.0045	438.696	457.74	C
Vs13	15	0.013795	1.0263	454.969	551.67	C
Vs14	7	0.042062	1.0292	330.811	431.73	C
Vs15	11	0.02214	1.0341	350.646	450.60	C

southeast by approximately 800 km along the Red River and three Pagoda fault zones during the first 20-30 million years of a collision. Transtension is occurred as one of the present tectonic stress regimes in Thailand and Laos, with an opening along north-south oriented basins and right-lateral and left-lateral slip on the northwest and northeast-striking faults, respectively (Polachan et al., 1991; Packam, 1993).

3.1. Crustal Faults

Thailand has 27 active fault systems located in and near the country area (Warnitchai, 2010) which are mainly obtained from recent paleo-seismic investigations discovered by Woodward-Clyde Federal Services in Northern Thailand (TDMR, 1996), Western Thailand (EGAT 1998), and Southern Thailand (RID 2005). Seismicity surrounding the site is considered by several significant faults such as Mae Chan, Mae Ing and Phayao faults as shown in Figures 6 and 7. All of the above faults are left-lateral strike-slip except southern segments of Phayao fault. Mae Chan fault with a length of 118 km and the slip rate of 0.3 to 3 mm/yr has a maximum credible earthquake (MCE) M_w of 7.5. Mae Ing fault with the length of 38 km and the slip rate of 0.3 to 1.2 mm/yr has (MCE) Mw 7.4, and Phayao fault with the length of 100 km and the slip rate of 0.1 mm/yr can create Mw of 6.8.

Figure 6. Seismic hazard map of Thailand (a) Seismicity in the study region M_w>3 within 100 years from 1917 to 2017 Clustered from USGS (USGS 2015 and TMD catalogs (TMD, 2015), (b) A Seismic hazard zoning map of Thailand based on information from Department of Mineral Resources, The Meteorological Department, and National Earthquake Information Center (USA)

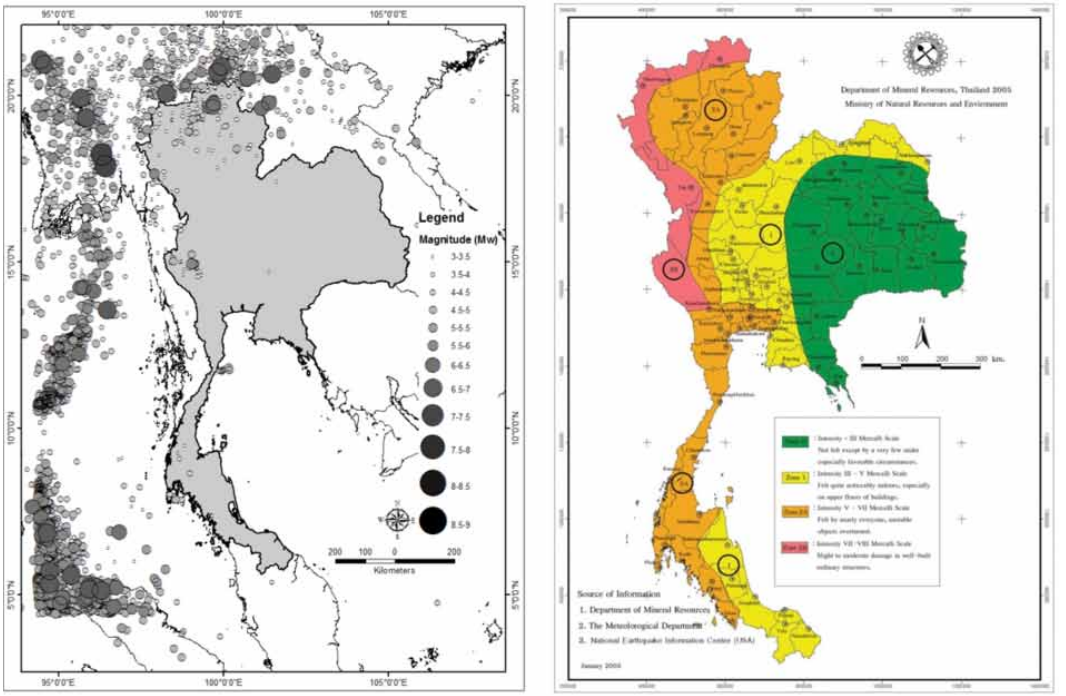

The grey circles are the earthquakes before the Chiang Rai mainshock (prior to 5 May 2014), and the red circles are the mainshock and aftershocks till late 2015. With the different sizes of circles representing the magnitude scales. The solid dark blue lines are active faults mapped by TDMR (2016). The heavy blue lines denote the Thailand border. The dashed box represents the Mae Lao area.

Figure 7. Seismicity of northern Thailand and surrounding regions, including Myanmar and Laos (Pananont et al., 2017)

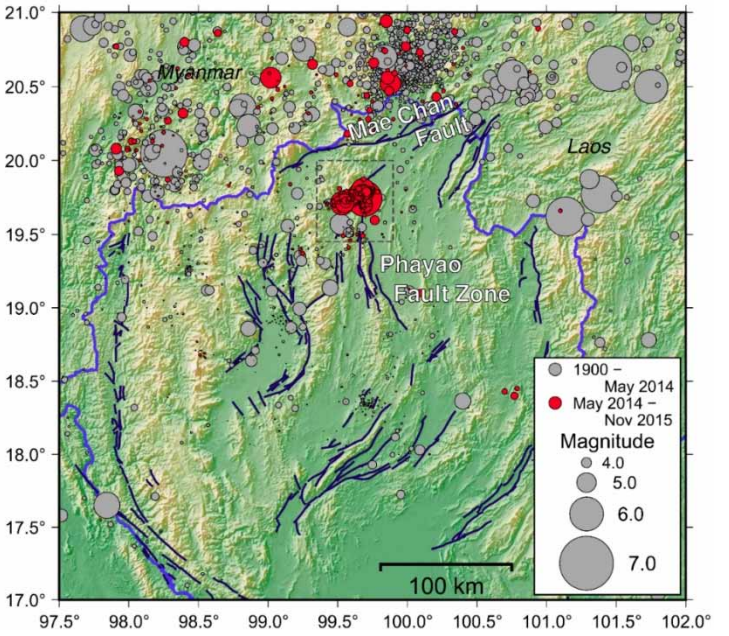

Nearly 1000 aftershocks were recorded by the regional and temporary seismic networks between May 5, 2014, and April 14, 2015, with 160 aftershocks of magnitudes up to M_L 5.3 within the first 24 h following the mainshock. Based on the aftershock activity, along the NNW-SSE trend, the initial fault rupture zone of this earthquake approximated 10 to 15 km in length, consistent with the expected length of ~10 km for earthquakes of this magnitude (Coppersmith, 1994).

In order to analyze the seismic hazard, the closest active fault i.e. Phayao fault is considered as the cause of the 6.2 M_w Chiang Rai earthquake in 2014 that has a high effect on the seismic hazard of the study area. Fifteen boring logs were observed surrounding Phayao fault (Figure 8) and have a

Figure 8. Location of the study area to the closest active faults, modified from Google Earth (GERD, 2014)

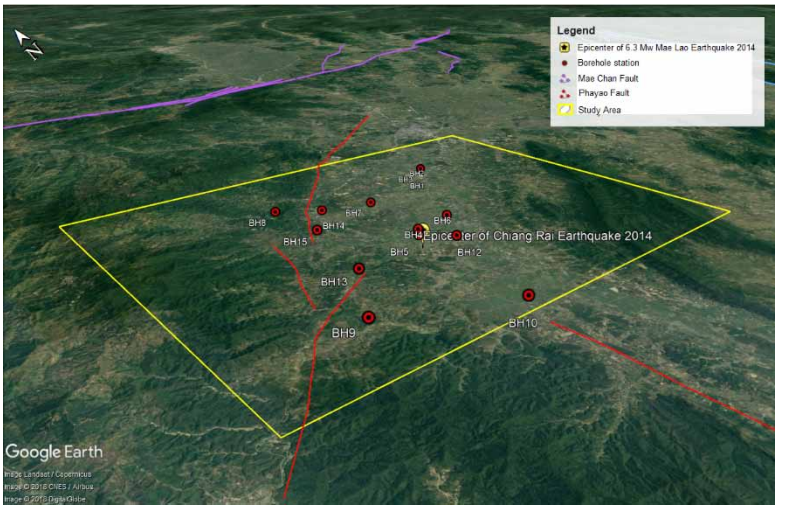

very close distance to the sites especially for Borehole BH4, BH5, and BH12 that only about 1 km away from the epicenter. Station BH5 has the closest distance of 0.671 km and BH11 as the farthest distance of 22.08 km to the epicenter, respectively.

3.2. Estimation of Ground Motion Parameters

Thai Meteorological Department (TDMR, 2015) revealed a moderate strike-slip was triggered by the Phayao Fault and was the second-largest earthquake in Thailand after the M_w 6.3 Nan Earthquake (Nan Province) in 1935. There are several seismic stations (Figure 8) that recorded the ground motion of the Chiang Rai earthquake, as compiled in Table 3. The ground motion parameter is obtained from Thai Meteorological Department (TDMR, 2015) including the peak ground acceleration on the vertical and horizontal directions (PGA_v and PGA_h), peak ground velocity (PGV), effective duration (D5-95), and the distance to surface projection of the rupture surface (Jorner-Boore distance (R_{jb})). The maximum horizontal acceleration (PGA_h) of 0.3g was recorded at MSAC station (Mae Suai station) which is 14 km to the southeast of the earthquake epicenter.

Figure 9. The regional seismic station recorded Chiang Rai earthquake ground motion, modified from Google Earth

In order to estimate the ground motion in the study are, the ground motion prediction (GMP) analysis is performed using the Next Generation Attenuation model 2014 (NGA-West2). The result of predicted PGA from the analysis then to be considered in the CSR calculation to determine the liquefaction potential value as well as the susceptibility associates with the geological criteria as presented in Table 4.

The analysis is done by considering the Mae Lao earthquake information related to the source mechanism, the magnitude of the earthquake, site to source distance, and other seismological

Table 3. Recorded ground motion from the accelerometer of Chiang Rai earthquake 6.2 M_w 2014

Stations	Location		NEHRP class	V_{S30} (m/s)	R_{jb} (km)	Source to Site Azimuth (deg)	Ground Motion Parameters			
	Lat	Long					PGA_h	PGV	PGA_v	D_{5-95}
	(N)	(S)					(g)	(m/s)	(g)	(s)
MSAC	19.679	99.536	B	780	14	234	0.3	21.6	0.21	4.5
MACR	19.675	99.928	D	300	25	116	0.13	2.8	0.09	13.5
MEAJ	20.146	99.852	D	300	38	20	0.04	2.5	0.02	19.5
PAYA	19.36	99.869	C	360	48	160	0.06	3.5	0.03	5.5
POPY	19.17	100.283	D	300	85	135	0.03	2.4	0.01	31
CDCM	19.409	98.982	C	360	85	244	0.03	2.7	0.01	10.5
NGLP	18.785	99.938	D	300	112	164	0.02	2.7	0.008	28
CHTO	18.808	98.96	B	780	129	217	0.01	0.2	0.01	9.7
LAMP	18.517	99.632	B	780	132	183	0.005	0.35	0.003	13
NAN	19.303	100.89	D	300	136	111	0.01	0.9	0.005	36
SMCM	18.853	98.739	C	360	139	225	0.04	1.6	0.02	15
PHRA	18.493	100.225	C	360	142	158	0.005	0.7	0.003	24
LUMP	18.566	99.038	D	300	150	208	0.02	1.6	0.01	50
PHEA	18.127	100.165	C	360	185	164	0.01	1.5	0.002	80
MJCM	18.501	98.373	C	360	194	225	0.02	2.7	0.01	25

Table 4. Evaluation of liquefaction hazard associates to the geological criteria (according to Bachuber, 2008), groundwater level, and predicted PGA

Stat.	Geologic unit	Evidence	G.W.L.	Coordinates		Distance (km)	Predicted PGA (g)	Liquefaction Hazard
				Lat. (ºN)	Long. (ºE)			
BH1	Q_{ff}	No	1.74	19.82421	99.76320	11.212	0.23	Low
BH2	Q_{ff}	No	1.74	19.82421	99.76289	11.212	0.23	Low
BH3	Q_{ff}	No	1.74	19.82451	99.76310	11.212	0.23	Low
BH4	Q_a	Yes	0.96	19.75961	99.69688	1.400	0.49	High
BH5	Q_a	Yes	1.56	19.75439	99.69211	0.671	0.50	High
BH6	Q_a/Q_{ff}	Yes	1.18	19.76337	99.72059	3.441	0.41	High
BH7	Q_a	Yes	-1.55	19.79962	99.70361	5.809	0.34	High
BH8	CP	No	-4.57	19.81991	99.65781	8.700	0.28	Low - None
BH9	SD	Yes	-3.425	19.71367	99.62831	7.725	0.30	Low-None
BH10	Q_t	Yes	-1.86	19.68779	99.68379	3.478	0.41	Moderate
BH11	Q_a	Yes	-2.725	19.64923	99.50963	22.080	0.13	Moderate
BH12	Tr	No	-1.65	19.74342	99.70494	1.433	0.51	Low-None
BH13	CP/Q_a	No	-0.47	19.74404	99.66323	3.030	0.43	Low-None
BH14	Q_t	No	-3.84	19.80651	99.67614	6.646	0.32	Moderate
BH15	CP/Q_t	No	-7.99	19.78741	99.65978	5.465	0.36	Low-None

conditions of the study area. Other than that, the local site condition represented by Vs_{30} of the site was also used as the input parameter. Every information is used to estimate the ground motion values relying on the actual distance and local site condition then compared to the recorded ground motion. NGA-West2 was developed by five models including Abrahamson, Silva, and Kamai (Abrahamson et al., 2014), Boore, Stewart, Seyhan, and Atkinson (Boore et al., 2014), Campbel and Bozorgnia (Campbel & Bozorgnia, 2014), Chiou and Youngs (Chiou & Youngs, 2014), and Idriss (Idriss, 2014). Based on the model applicability, Idriss required the model only for a very dense to Rock soil class which have V_{S30} value of more than 450 m/s. The weighting value for each of the four other models is 0.25 and averaged by geometric of the natural logarithm of the spectral values. The damping ratio is 5% with the damping scaling factor (DSF) of 1.

Other than site classes, source-to-site distance plays an important role in determining the susceptibility of liquefaction that relates to the ground amplification. In general, earthquake shaking decreases with distance away from the earthquake source. soft soil can increase the level and duration of shaking depending on the proximity of the earthquake and can affect how the structure may react such as liquefaction. Therefore, the site amplification has been illustrated by 1D EQL Deepsoil to determine the ground response which leads to the susceptibility of liquefaction.

4. LIQUEFACTION SUSCEPTIBILITY ASSESSMENT

Consideration of site-specific engineering properties of soils and site conditions is a key aspect in the evaluation of liquefaction potential at a certain site (Maurer et al., 2014). Initially, screening the procedures based on soil classification (soil composition) and geological criteria are often adopted to examine whether the soil at the site is susceptible to liquefaction or not.

4.1 Liquefaction Susceptibility Based-Compositional Criteria

The susceptibility of liquefaction can be evaluated with the geotechnical soil properties like the percentage of fine content, Atterberg limits, water content, and grain size distribution of soil (Seed & Idriss 1982). The liquefaction susceptibility analysis is divided into 2 groups: liquefaction susceptibility of fine-grain soil and liquefaction susceptibility of sandy soil. Liquefaction susceptibility analysis of fine-grain soil can be done by using criteria that were proposed by Bray & Sancio (2006), Andrews & Martin (2000), and Seed & Idriss (1982). Seed and Idriss (1982) proposed the evaluation of potentially liquefiable soils (Chinese criteria) that had been widely used for many years. According to these criteria, the fine-grained soils are considered to be potentially liquefiable if the fraction finer 0.005 mm is less than 15%, Liquid Limit of £ 35%, and water content greater than or equal to 90% of the Liquid Limit. Besides, based on the plasticity chart it was recommended to use new criteria from case histories and cyclic testing of undisturbed fine-grained soils (Seed et al., 2003). These criteria have been classified into 3 liquefaction zones: soil within Zone A are considered potentially susceptible to cyclically-induced soil liquefaction, soils within Zone B fall into a transition range; they may in some cases be susceptible to liquefaction (especially if in situ water content is greater than about 85% of their Liquid Limit), and soils in Zone C are generally not susceptible cyclically-induced soil liquefaction. In contrast, Bray & Sancio (2006) presented the new criteria that even fine-grained soils that can demonstrate susceptibility to liquefaction or cyclic mobility for the soils with a plasticity index (PI) > 18 and wc/LL > 0.8. Finally, the evaluation of liquefaction susceptibility by Seed and Idriss (1982) was carried out for each soil layer for all stations.

Figures 10 and 11 represent the grain size distribution of every layer of soil at station BH-10 which dominantly consists of sand. Most of the gradation curves are placed in between inner thick lines (most liquefiable soil) and some in between the inner and outer lines (potentially liquefiable soil). It can be concluded that those layers are highly susceptible to liquefaction. From the analysis using soil distribution method of 15 boreholes, it can be observed that most of the sample have a layer of sandy soils and hence are susceptible to liquefaction.

Figure 10. Compositional soil gradation and liquefaction susceptibility of BH-10

Depth (m)	Soil	USCS	Distribution of soil	FC (%)	% Clay (%)	Corrected SPT	Plasticity of silty soil (PI)	Plasticity of silty soil (LL)	Liquefaction Susceptibility
0 1		CL	-	79.27	22.66	7	9.98	30.59	Potentially Liquefiable
2		SM	Uniform grade	23.70	5.24	9			Liquefiable
3		SP-SM	Uniform grade	5.20	-	22			Liquefiable
4		SW-SM	Well grade	8.56	-	17			Potentially Liquefiable
5		SW-SM	Well grade	11.00	2.07	18			Potentially Liquefiable
6		SP	-	-	-	20			Liquefiable
7		SP	Uniform grade	5.50	-	12			Liquefiable
8		SW-SM	Uniform grade	6.80	-	12			Liquefiable
9		SW-SM	Well grade	5.45	1.20	13			Potentially Liquefiable
10		SW-SM	Uniform grade	11.71	-	36			Potentially Liquefiable
11		SW-SM	-	7.76	-	57			Non Liquefiable
12		SP	Well grade	34.05	8.61	100			Non Liquefiable
13		SP	-	13.41	-	100			Non Liquefiable

4.2 Liquefaction Susceptibility Based-Geologic Criteria

One of the important steps in assessing a liquefaction susceptibility is by identifying the geologic deposit through age and textural characteristics are most susceptible to liquefaction (Bachuber et al., 2008). The area with poorly engineered hydraulic fills and late Holocene fluvial has the most liquefiable deposits (Pyke, 2003). In this study, the Quaternary and the geomorphologic mapping (Figure 3) identified the latest Holocene deposits of the fan, terrace, and alluvium which have low, and medium to high liquefaction potential relating to ground motion. The liquefaction potential is

Figure 11. Liquefaction susceptibility assessment of BH-10 for every layer of soil using grain size distribution curve (adapted from Tsuchida 1970) analysis

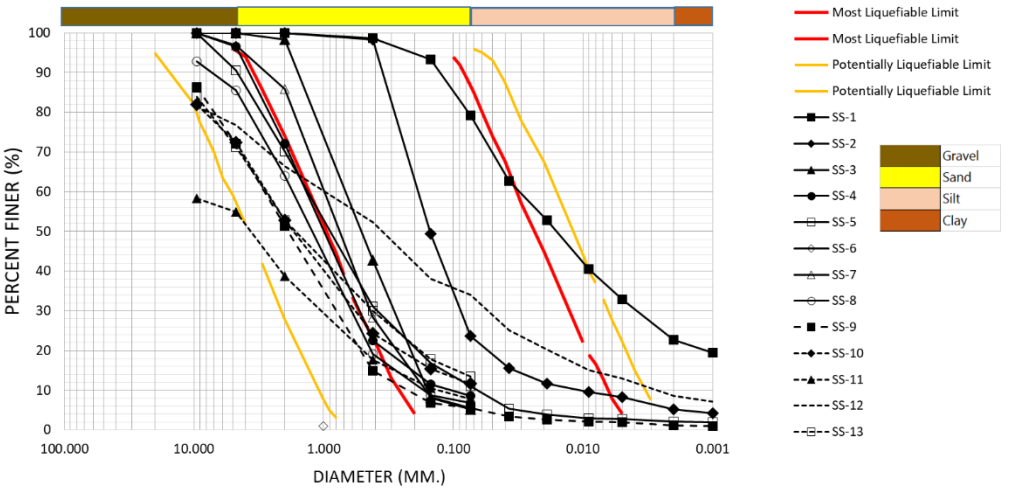

classified and tabulated based on geologic types relating to the groundwater level and predicted ground motion. Using the combination of them, the liquefaction hazard by the geologic condition can be determined as presented in Table 4.

Bachhuber *et al.* (2008) in their study revealed that the high susceptibility of liquefaction consists of late Holocene alluvial (Q_a) and Holocene beach deposits (Q_b) which dominantly comprises of sand and silty sand (estimated sand and silt percentages less than 80%), and occurred in low areas with a relatively high groundwater level typically less than 1.5 meters deep. The Qa unit is assigned as a high potential of liquefaction susceptibility rating with a PGA triggering threshold of 1.0 to 0.15g and the Q_b as a medium-to-high potential of liquefaction susceptibility rating with a PGA of 0.1 to 2.0 g. In this study, the geologic Q_a unit is placed in the area of BH4, BH5, BH6, BH7, and BH11. Most of these Qa deposits claimed as a high potential of susceptibility showing the evidence of liquefaction from 6.2 M_w Chiang Rai earthquake. Also, regards to the estimated PGA which is capable to trigger the liquefaction in these areas.

Late Pleistocene to Holocene Terraces (Q_t) is classified as a medium susceptibility to liquefaction that typically consists of interbedded clay, silt and sand with gravel lenses (liquefiable texture 35 to 50%), and the estimated PGA triggering threshold of 0.15 to 0.25g with the groundwater level ranging from about 1.5 to 6 meters depth. The geologic map shows that the Q_t deposit is located on BH10 and BH14. Even though this type of deposit is classified as a medium susceptibility, the BH10 in this study indicated a high susceptibility of liquefaction considering the compositional criteria of the boring log which was dominantly composed by sand layer and the significant evidence of liquefaction in this area.

Furthermore, the Quaternary of flood plain (Q_{ff}) which represents the Pleistocene-aged alluvial fan deposits located at the valley area that consists of well-graded clayey gravel sediment has a Low to medium and Low susceptibility of liquefaction. The liquefiable texture is about 10 to 30 percent with a groundwater level of about 1.5 to 10 meters. BH1-BH3 and BH6 are the Q_{ff} deposits that have low susceptibility of liquefaction and are suitable for the result of the cyclic stress approach (Seed et al. 1985). Other than that, the very low-to-negligible chance of liquefaction classifies for siltstone, sandstone, and basic rock (Tr, CP, and SD) located on BH8, BH9, BH13, and BH15, respectively.

4.3 Liquefaction Potential Based on Liquefaction Potential Index (LPI) Value

Safety factor against liquefaction (FS_L) for each layer was calculated using the simplified method of soil liquefaction analysis as proposed by Seed and Idriss (1971). After the FS_L was established, the Liquefaction potential index (LPI) could be estimated using the formula suggested by Iwasaki et al. (1982) as in equation 7 is known as the cyclic stress approach. All the borehole profiles were defined and classified to every level of severity according to the total LPI value of each layer per boreholes:

$$FS_{liq} = \frac{CRR_{M,\sigma'_{vc}}}{CSR} \tag{2}$$

$$CRR_{M=7.5} = \exp\left(\frac{(N_1)_{60cs}}{14.1} + \left(\frac{(N_1)_{60cs}}{126}\right)^2 - \left(\frac{(N_1)_{60cs}}{23.6}\right)^3 + \left(\frac{(N_1)_{60cs}}{25.4}\right)^4 - 2.8\right) \tag{3}$$

$$CRR_{M,\sigma'_{vc}} = CRR_{M=7.5,\sigma'_{vc}=1} \cdot MSF \tag{4}$$

$$MSF = \left(\frac{M_w}{7.5}\right)^{2.56} \tag{5}$$

$$CSR = 0.65\frac{\sigma_v}{\sigma'_v} \cdot \frac{a_{\max}}{g} \cdot \gamma_d \tag{6}$$

where, FS_L = Factor safety against liquefaction; $CRR_{M,\sigma'vc}$ = scaled cyclic resistance ratio by the MSF value; CSR = cyclic stress ratio induced by earthquake; $CRR_{M=7.5,\sigma'vc=1}$ = cyclic resistance ratio for earthquake M_w 7.5; $(N_1)_{60cs}$ = SPT blow count normalized to an over-burden pressure of approximately 100 kPa (1 ton/sq-ft) and a hammer energy ratio of 60%; MSF = magnitude scaling factor based on considered magnitude; σ_v = total overburden pressure in subsoil layers (t/m^2); σ'_v = effective overburden pressure in subsoil layers (t/m^2); g = gravity's acceleration (m/s^2); a_{max} = peak horizontal acceleration (m/s^2); γ_d = stress reduction factor.

Liquefaction potential index (LPI) is a single-valued parameter to characterize the damage of potential of liquefaction by integrating the factor of safety against liquefaction (FS_L) along with the soil column up to 20 m depth. The level of severity (Table 5) based on 1-dimensional analysis and cyclic stress approach by Iwasaki (1982) has been checked with the compositional criteria method for liquefiable soils. Ultimately, the comparison of both methods is verified and controlled by the eyewitness evidence of the liquefaction in the field.

The severity of liquefaction potential is defined by the LPI value (Iwasaki, 1982) expressed in equation 7 and presented in Table 6.

$$LPI = \int_0^{20} F.w(z)dz \tag{7}$$

where z is the depth of midpoint of the soil layer (0 to 20 m), dz is the differential increment of depth, w(z) and F(z) are weighting and severity factors, respectively:

Table 5. Level of severity based LPI value

Station / Borehole	Liquefiable Behavior (based on compositional criteria)	Liquefaction evidence (eyewitness)	LPI value		Level of severity	
			1D site response (DEEPSOIL)	Iwasaki (1982)	1D site response (DEEPSOIL)	Iwasaki (1982)
1	Potentially liquefiable	No	0.982	0.000	Low	None
2	Potentially liquefiable	No	2.872	0.000	Low	None
3	Potentially liquefiable	No	3.793	2.625	Low	Low
4	Liquefiable	Yes	15.710	9.307	High	Moderate
5	Liquefiable	Yes	8.984	5.307	Moderate	Low
6	Liquefiable	Yes	7.520	3.943	Low	Low
7	Liquefiable	Yes	9.156	4.971	Moderate	Low
8	Non liquefiable	No	0.000	0.000	None	None
9	Potentially-liquefiable	Yes	9.766	6.220	Moderate	Low
10	Liquefiable	Yes	23.136	14.290	High	Moderate
11	Liquefiable	Yes	21.933	13.089	High	Moderate
12	None liquefiable	No	1.286	0.000	Low	None
13	None liquefiable	No	0.000	0.000	None	None
14	None liquefiable	No	0.000	0.000	None	Low
15	None liquefiable	No	0.000	0.000	None	None

Table 6. Liquefaction potential classification by several methods

Liquefaction Potentials (severity)	Iwasaki (1982)	Sonmez (2003)	Maurer et al. (2014)	Kang et al. (2014) study	
				Chinese criteria	Bray-Sancio criteria
Little to None	LPI = 0	LPI = 0	LPI < 4	LPI = 0	LPI = 0
Low (Minor)	0 < LPI < 5	0 < LPI < 2	4 ≤ LPI < 8	0 < LPI < 11	0 < LPI < 14
Moderate	5 ≤ LPI < 15	2 ≤ LPI < 5	8 ≤ LPI < 15	11≤ LPI < 15	14 ≤ LPI < 21
High (Severe)	15 ≤ LPI ≤ 100	5 ≤ LPI < 15	>15	15 ≤ LPI ≤ 100	21 ≤ LPI ≤ 100
Very High	-	LPI > 15	-	-	-

$$F_i = 1 - FS_i \text{ for FSi} < 1.0 \tag{8}$$

$$F_i = 0 \quad \text{for FSi} \geq 1.0 \tag{9}$$

$$w(z) = 10 - 0.5z \text{ for z<20m} \tag{10}$$

$$w(z) = 0 \text{ for z>20m} \tag{11}$$

$$P_G = \left(3 \times 10^{-5}\right) LPI^3 - \left(0.0025\right) LPI^2 + \left(0.0756\right) LPI + 0.0879 \quad (12)$$

$$P_G = \left(3 \times 10^{-5}\right) LPI^3 - \left(0.0027\right) LPI^2 + \left(0.0746\right) LPI + 0.2977 \quad (13)$$

Maurer et al. (2014) evaluated the performance of LPI value using the cumulative distribution functions (CDFs) in predicting the occurrence and severity of surficial liquefaction manifestation based on nearly 1,200 sites observation. Finally, they came up with Equation 12 for the lower bound and equation 13 for the upper bound. By using these formulae, the probability of liquefaction manifestation (P_G) can be established. As shown in Figure 12 the P_G value tends to increase with the increasing LPI. The P_G £ 0.4 fall into low P_G value and were found at station BH1, BH2, BH3, BH8, BH12, BH13, BH14, and BH15. While the other stations have P_G ranging from 0.62 to 0.91 by 1D analysis and 0.45 to 0.82 by cyclic stress approach, respectively.

Figure 12. Liquefaction potential index and the probability of liquefaction manifestation (P_G)

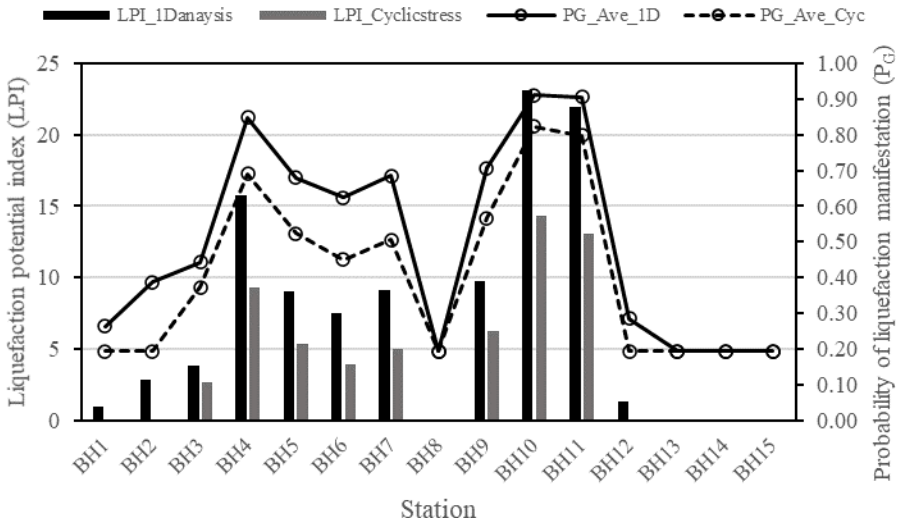

Moreover, a multi-layer ground response analyses have been done by Deepsoil 6.1 software (Hashash et al., 2016) using 1D Equivalent Linear Model (EQL) or known as frequency domain which considers shear damping (G/G_{max}) and damping ratio (%) to be defined as functions of shear strain (%). The bedrock type of analysis is applied as a rigid half-space which a within motion has been used. Hence, for the shaking analysis, ground motions have been obtained and selected from PEER database follows the assessed seismological characteristic, this ground motion parameters have been through scaling and matching processes before applied into the analysis. The default effective shear strain ratio of 0.65 is applied. Finally, the result leads to the LPI value to classify the severity of liquefaction potential and compared with other methods as presented in Table 5.

4.4 Correlation of Geological Characteristic and LPI Value

To classify the severity of liquefaction, several methods such as compositional criteria, geological type, and LPI value have been widely used. It is necessary to combine all the factors causing liquefaction susceptibility to verify and obtain the best result to conclude the severity of liquefaction event.

Figure 13 shows the trend of correlation between the LPI value and geological condition with respect to the compositional characteristic. Each blue column is LPI based on 1D EQL model by Deepsoil 6.1 analysis, and each yellow column is the LPI based on the cyclic stress approach. It clearly described that a deposit soil of Q_a has a higher potential of liquefaction due to the depositional structure and the LPI value compared to other units. Although Q_t in the geologic unit is classified as a moderate level of severity, one of the data in BH11 shows the behavior of the high potential of liquefaction. Considering both geological characteristics and LPI computation, the Q_t unit of Mae Lao District could be classified as the moderate-to-high potential of liquefaction. Moreover, the geologic units of Q_{ff}, tr, SD, and CP have low to no potential to cause liquefaction. Eventually, the result of liquefaction potential is classified in four categories of severity which are none, low, moderate, and high, considering the geological criteria and LPI analysis by Deepsoil 6.1. On the other hand, the liquefaction severity by cyclic stress approach does not have a high level and only falls into those three categories. Between the two LPI assessment methods, the 1D EQL model likely overrates the potential of liquefaction and has averagely two times LPI value compared to the cyclic stress method. The field evidence most likely into the category based on cyclic stress approach from low to moderate level of severity.

Figure 13. Correlation between LPI value and the geological type

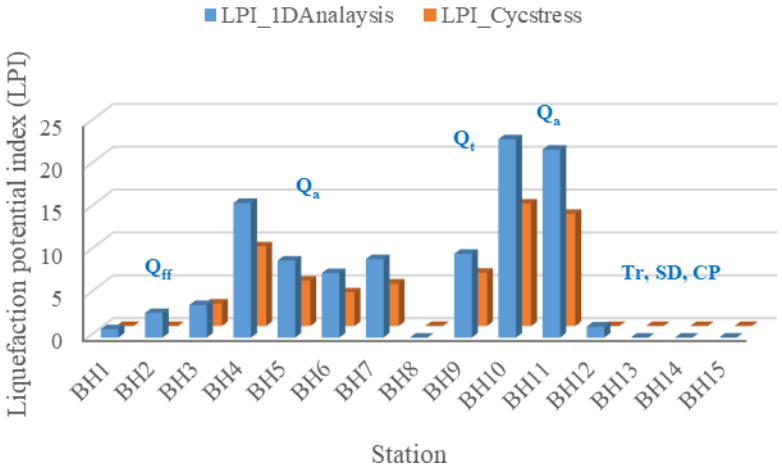

5. CONCLUSION

The geological and geotechnical aspects of the study area have a complex formation that consists of depositional materials of clay, silt, sand, gravel, siltstone, etc. Moreover, Late Holocene alluvial (Q_a), Late Pleistocene to Holocene Terraces (Q_t), Pleistocene-aged alluvial fan deposits (Q_{ff}), and the Siltstone and Sandstone (Tr, CP, and SD) laid on the study area that governs the variation of liquefaction behavior. The study of groundwater level (observation well) within a period of one year has identified the area with high groundwater level fluctuating over time. These several factors were combined to generate a suitable prediction of liquefaction susceptibility.

Quaternary deposit of Alluvium (Q_a) is considered to be moderate-to-high susceptibility of liquefaction based on the depositional criteria. The result was also verified after the liquefaction potential index (LPI) values were established using the cyclic stress approach and the 1D EQL method. The LPI value of Q_a in this study generally ranging from 8 to 23, and classified as moderate-to-high potential of liquefaction. Furthermore, it suits the evidence that occurred after the earthquake 6.2 M_w

Chiang Rai earthquake 2014. The liquefaction evidence such as sand boiling were observed within 10 km from the epicenter which laid on the Holocene alluvial and alluvial fan deposits. Hence, distance affects the time travel of energy source which leads to ground amplification causes a high potential of liquefaction in the area. Moreover, the groundwater level fluctuation also supports the judgment of both criteria (Geological and LPI) and it is found to be a high groundwater level and fluctuating over the year which is prone to have a high chance of liquefaction. On another hand, the area with no liquefaction evidence has low-to-none susceptibility of liquefaction. This area is located on the rock-site area such as Siltstone and Sandstone which have no possibility of liquefaction (negligible). Eventually, geotechnical and geological factors combined to assess the liquefaction potential are suitable to support each other aspects and for better judgement that associates with the design of liquefaction hazard for a specified study area.

ACKNOWLEDGMENT

The authors would like to thank the Civil Engineering Department, Faculty of Engineering, Kasetsart University for the full master scholarship, grateful thanks to Geotechnical Engineering Research and Development (GERD) Center, and to Thailand Research Fund for providing the research and available data.

REFERENCES

Abrahamson, N. A., Silva, W. J., & Kamai, R. (2014). Summary of the ASK14 ground-motion relation for active crustal regions. *Earthquake Spectra*, *30*(3), 1025–1055. doi:10.1193/070913EQS198M

Ammon, J., Ji, C., Thio, H., Robinson, D., Ni, S., Hjorleifsdottir, V., Kanamori, H., Lay, T., Das, S., Helmberger, D., Ichinose, G., Polet, J., & Wald, D. (2005). Rupture process of the 2004 Sumatra-Andaman. *Earth Science*, *308*(1), 1133–1139. doi:10.1126/science.1112260 PMID:15905393

Andrews, D. C. A., & Martin, G. R. (2000). Criteria for Liquefaction of Silty Soils. *Proc. of 12th World Conference on Earthquake Engineering*.

Bachhuber, J. L., Hengesh, J. V., & Sundermann, S. T. (2008). *Liquefaction Susceptibility of the Bayamon and San Juan Quadrangles, Puerto Rico. United States Geological Survey*. USGS.

Boore, D. M. (2004). Estimating VS30 (or NEHRP site classes) from shallow velocity models (depth < 30 m). *Bulletin of the Seismological Society of America*, *94*(2), 591–597. doi:10.1785/0120030105

Boore, D. M., Stewart, J. P., Seyhan, E., & Atkinson, G. M. (2014). NGA-West2 equations for predicting PGA, PGV, and 5% damped PSA for shallow crustal earthquakes. *Earthquake Spectra*, *30*(3), 1057–1085. doi:10.1193/070113EQS184M

Boore, D. M., Thompson, E. M., & Cadet, H. (2011). Regional correlations of VS30 and velocities averaged over depths less than and greater than 30 m. *Bulletin of the Seismological Society of America*, *101*(6), 3046–3059. doi:10.1785/0120110071

Bray, J. D., & Sancio, R. B. (2006). Assessment of the liquefaction susceptibility of fine-grained soils. *Journal of Geotechnical and Geoenvironmental Engineering*, *132*(99), 1165–1177. doi:10.1061/(ASCE)1090-0241(2006)132:9(1165)

Campbell, K. W., & Bozorgnia, Y. (2014). NGA-West2 Ground Motion Model for the Average Horizontal Components of PGA, PGV, and 5% Damped Linear Acceleration Response Spectra. *Earthquake Spectra*, *30*(3), 1087–1115. doi:10.1193/062913EQS175M

Chiou, B. S. J., & Youngs, R. R. (2014). Update of the Chiou and Youngs NGA model for the average horizontal component of peak ground motion and response spectra. *Earthquake Spectra*, *30*(3), 1117–1153. doi:10.1193/072813EQS219M

EGAT. (1998). *Electricity Generating Authority of Thailand*. Preliminary Seismic Hazard Evaluation of Khao Laem and Srinagarind Dams.

Geotechnical Engineering Research and Development Center (GERD). (2014). *Dataset borehole of Mae Lao District*. Geotechnical Engineering Research and Development.

Geotechnical Engineering Research and Development Center (GERD). (2020). *Elevation Map of Thailand*. Geotechnical Engineering Research and Development.

Hashash, Y. M. A., Musgrove, M. I., Harmon, J. A., Groholski, D. R., Phillips, C. A., & Park, D. (2016). DEEPSOIL 6.1 User Manual. Academic Press.

Idriss, I. M. (2014). An NGA-West2 empirical model for estimating the horizontal spectral values generated by shallow crustal earthquakes. *Earthquake Spectra*, *30*(3), 1155–1177. doi:10.1193/070613EQS195M

Iwasaki, T., Tokida, K., Tatsuoka, F., Watanabe, S., Yasuda, S., & Sato, H. (1982). Microzonation for soil liquefaction potential using simplified methods. *Proceeding of the 3rd International Conference on Microzonation*, 1319–1330.

Kang, G. C., Chung, J. W., & David, J. R. (2014). Re-calibrating the thresholds for the classification of liquefaction potential index based on the 2004 Niigata-ken Chuetsu earthquake. *Engineering Geology*, *169*, 30–40. doi:10.1016/j.enggeo.2013.11.012

Maurer, B. W., Russell, A. G. M., Cubrinovski, M., & Bradley, B. A. (2014). Evaluation of the liquefaction potential index for assessing liquefaction hazard in Christchurch, New Zealand. *Journal of Geotechnical and Geoenvironmental Engineering*, *140*(7), 04014032. Advance online publication. doi:10.1061/(ASCE)GT.1943-5606.0001117

McCaffrey, R. (1996). Slip partitioning at convergent plate boundaries of south East Asia in Tectonic Evolution of Southeast Asia. Geological Society of London.

Ornthammarath, T., & Warnitchai, P. (2016). 5 May 2014 Mw.6.1 Mae Lao (Northern Thailand) earthquake: Interpretations of recorded ground motion and structural damages. *Earthquake Spectra*, *32*(2), 1209–1238. doi:10.1193/081814eqs129m

Pakcham, G. H. (1993). Plate tectonics and the development of sedimentary basins of the dextral regime in Western Southeast Asia. *Journal of Southeast Asian Earth Sciences*, *8*(1–4), 497–511.

Pananont, P., Herman, M. W., Pornsopin, P., Furlong, K. P., Habangkaem, S., Waldhauser, F., Wongwai, W., Limpisawad, S., Warnitchai, P., Kosuwan, S., & Wechbunthung, B. (2017). Seismotectonics of the 2014 Chiang Rai, Thailand, earthquake sequence. *Journal of Geophysical Research. Solid Earth*, *122*(8), 6367–6388. Advance online publication. doi:10.1002/2017JB014085

Polachan, S., Pradidtan, S., Tongtaow, C., Janmaha, S., Intarawijitr, K., & Sangsuwan, C. (1991). Development of cenozoic basins in Thailand. *Marine and Petroleum Geology*, *8*(1), 84–97. doi:10.1016/0264-8172(91)90047-5

Pyke, R. (2003). Discussion of liquefaction resistance of soils: Summary report from the 1996 NCEER and 1998 NCEER/NSF workshops on evaluation of liquefaction resistance of soils. *Journal of Geotechnical and Geoenvironmental Engineering*, *129*(3), 283–284. doi:10.1061/(ASCE)1090-0241(2003)129:3(283)

Royal Irrigation Department of Thailand. (2005). Seismic Hazard Evaluation of the Tha Sae Project, Thailand. URS Corporation.

Seed, H. B., Cetin, K. O., Moss, R. E. S., Kammerer, A. M., Wu, J., Pestana, J. M., Riemer, M. F., Sancio, R. B., Bray, J. D., Kayen, R. E., & Faris, A. (2003). Recent advances in soil liquefaction engineering: a unified and consistent framework. *Proceeding of the 26th Annual ASCE L.A. Geotechnical Spring Seminar*.

Seed, H. B., & Idriss, I. M. (1971). Simplified procedure for evaluating soil liquefaction potential. *Journal of Soil Mechanic and Foundation Division, ASCE*, *97*(9), 1249–1273.

Seed, H. B., & Idriss, I. M. (1982). *Ground motion and soil liquefaction during earthquakes Monograph*. Earthquake Engineering Research Institute.

Seed, H. B., Tokimatsu, K., Harder, L. F., & Chung, R. M. (1985). Influence of SPT procedure in soil liquefaction resistance evaluations. *Journal of Geotechnical Engineering*, *111*(12), 1425–1445. doi:10.1061/(ASCE)0733-9410(1985)111:12(1425)

Sonmez, H. (2003). Modification of the liquefaction potential index and liquefaction susceptibility mapping for a liquefaction-prone area (Inegol, Turkey). *Environmental Geology*, *44*(7), 862–871. doi:10.1007/s00254-003-0831-0

Tangjittham, P. (2017). *Liquefaction Potential Assessment Using Spectral Analysis of Surface Waves Testing at Amphur Mae Lao, Chiang Rai, Thailand* (Master Thesis). Kasetsart University, Thailand.

Thai Department of Mineral Resources. (1990). Geological Map of Thailand. Author.

Thai Department of Mineral Resources. (1996). *Environmental impact assessment: geological aspect, Kaeng Sua Ten Dam project, Changwat Phrae.* Main Report No.3, Ministry of Industry Thailand.

Thai Department of Mineral Resources. (2015). Mae Lao Earthquake Data of Thailand in 2015. Bangkok, Thailand: Author.

Thai Department of Mineral Resources. (2016). *Thailand geological map*. Retrieved from http://www.dmr.go.th/n_more_news_en.php?nid=109504

Thai Meteorological Department. (2014). *Earthquake catalogue of Northern Thailand.* Retrieved from http://www.earthquake.tmd.go.th/earthquakestat.html

Thai Meteorological Department. (2015). Earthquake Report in Thailand and Adjacent countries in 2014. Seismological Bureau.

Tsuchida, H. (1970). Prediction and Countermeasure against Liquefaction in Sand Deposits. Abstract of the Seminar of the Port and Harbour Research Institute, Ministry of Transport, Yokosuka, Japan, 3(1), 3-33.

United States Geological Survey. (2015). *Earthquake catalogue of Thailand.* United State Geological Survey. Retrieved from https://earthquake.usgs.gov/earthquakes/search/

Warnitchai, P. (2010). Xayaburi Hydroelectric Power Project CH. Technical Report Karnchang (Lao) Company Limited.

Wells, D. L., & Coppersmith, K. J. (1994). New empirical relationships among magnitude, rupture length, rupture width, rupture area, and surface displacement. *Bulletin of the Seismological Society of America*, *84*(4), 974–1002.

Youd, T., & Perkins, D. (1978). Mapping liquefaction-induced ground failure potential. *Journal of Geotechnical Engineering*, *104*(4), 433–446.